Josef Malík; Alexej Kolcun

Determination of the initial stress tensor from deformation of underground opening – theoretical background and applications

In: Jan Chleboun and Pavel Kůs and Jan Papež and Miroslav Rozložník and Karel Segeth and Jakub Šístek (eds.): Programs and Algorithms of Numerical Mathematics, Proceedings of Seminar. Jablonec nad Nisou, June 19-24, 2022. Institute of Mathematics CAS, Prague, 2023. pp. 107–122.

Persistent URL: http://dml.cz/dmlcz/703193

Terms of use:

Institute of Mathematics of the Czech Academy of Sciences provides access to digitized documents strictly for personal use. Each copy of any part of this document must contain these *Terms of use*.

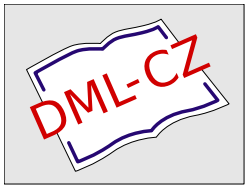

This document has been digitized, optimized for electronic delivery and stamped with digital signature within the project *DML-CZ: The Czech Digital Mathematics Library* http://dml.cz

Programs and Algorithms of Numerical Mathematics 21
J. Chleboun, P. Kůs, J. Papež, M. Rozložník, K. Segeth, J. Šístek (Eds.)
Institute of Mathematics CAS, Prague 2023

DETERMINATION OF THE INITIAL STRESS TENSOR FROM DEFORMATION OF UNDERGROUND OPENING — THEORETICAL BACKGROUND AND APPLICATIONS

Josef Malík, Alexej Kolcun

Institute of Geonics, The Czech Academy of Sciences
Studetská 1768, 708 00 Ostrava-Poruba, Czech Republic
josef.malik@ugn.cas.cz, alexej.kolcun@ugn.cas.cz

Abstract: In this paper a method for the detection of initial stress tensor is proposed. The method is based on measuring distances between some pairs of points located on the wall of underground opening in the excavation process. This methods is based on the solution of eighteen auxiliary problems in the theory of elasticity with force boundary conditions. The optimal location of the pairs of points on the wall of underground work is studied. The pairs must be located so that the condition number of a certain matrix has the minimal value, which guarantees a reliable estimation of initial stress tensor.

Keywords: initial stress tensor, first boundary value problem of the theory of elasticity, condition number of matrices

MSC: 65N30, 74-XX, 93E24

1. Introduction

The knowledge of initial stress tensor is very important when one evaluates the stability of underground openings like tunnels, compressed gas tanks or radioactive waste deposits. The knowledge of initial stress tensor enables to optimize the reinforcement of tunnels, choose the suitable shape of underground works and their orientation in the rock environment. The mathematical modeling of stress fields in the vicinity of underground openings requires precise boundary conditions, which can be derived from initial stress tensor. Extensive literature is devoted to the determination of initial stress tensor. An overview of these methods can be found in the papers [1]–[3] that describe the development of these methods to the present. Theoretical and practical aspects of these methods are studied in [4] and [5]. These methods are based on the installation of probes equipped with sensors that measure deformations occurring after removal rock, overcoring, in their vicinity. Due to the stress in the rock, the removal of a part of the rock causes deformation of the remaining rock, which is transfered to the sensors. The probes are relatively small, a few

DOI: 10.21136/panm.2022.11

centimeters, and the accuracy of such measurements is not high. A very interesting method that allows to determine the whole initial stress tensor is presented in [6].

In this paper we present a new method, which is based on measuring the distances between pairs of selected points on the walls of the underground work. When a part of the rock is excavated, the distance between these points changes and the magnitude of these changes depends on the initial stress tensor. A procedure which allows to determine the initial stress tensor from the measured distances is developed. A criterion showing how to select measuring points so that errors of measurement do not affect the results very much is presented. This method guarantees a reliable estimate of the initial stress tensor. The procedure of optimal choice of measuring points is based on the conditional number of the matrix corresponding with choice of measuring points.

2. Auxiliary results

The method described in this section is based on the solution of the first boundary problem of the theory of elasticity, e.i. only the force conditions are prescribed on the boundary of the domain, where the problem is solved. A typical problem solving domain is shown in Figure 1.

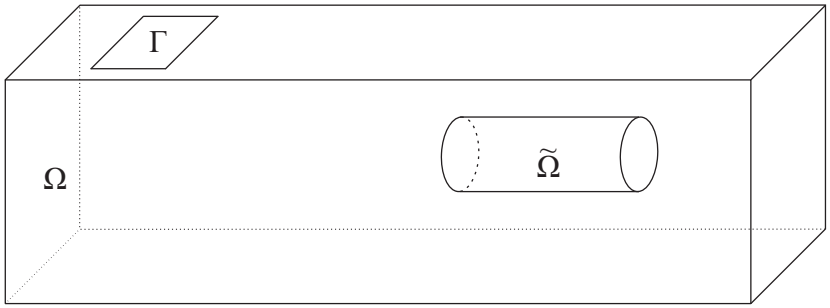

Figure 1: Typical problem solving area.

The symbol Ω in Figure 1 is the domain that corresponds to the prism and the symbol $\widetilde{\Omega}$ is the subdomain that represents the excavated space in the domain Ω. The symbol Ω_1 corresponds to domain $\Omega - \widetilde{\Omega}$ and $\Gamma \subset \partial\Omega$ has a nonzero measure. Let us have a space $V = [H^1(\Omega_1)]^3$, where $H^1(\Omega_1)$ is a Sobolev space of functions having first-oder derivatives that are integrable with the second power. We will continue to apply the Einstein summation convention.

Let us formulate the first variational problem $\mathcal{D}_1$ whose solution is a minimum of the following functional on V

$$\frac{1}{2}\int_{\Omega_1} c_{ijkl}e_{ij}(u)e_{kl}(u)\,\mathrm{d}x - \int_{\partial\Omega} P_i u_i\,\mathrm{d}S, \tag{1}$$

where $u = (u_1, u_2, u_3)$ belongs to V and

$$e_{ij}(u) = \frac{1}{2}\left(\frac{\partial u_i}{\partial x_j} + \frac{\partial u_j}{\partial x_i}\right)$$

is the tensor of small deformations. The symbol $P = (P_1, P_2, P_3)$ represents the forces on $\partial\Omega$ and $P_i \in L^2(\partial\Omega)$. The coefficient $c_{ijkl} \in L^\infty(\Omega_1)$ meet the following conditions

$$c_{ijkl} = c_{jikl} = c_{ijlk} = c_{klij}. \tag{2}$$

There is a constant $C > 0$ such that the inequality

$$c_{ijkl} e_{ij} e_{kl} \geq C e_{ij} e_{ij} \tag{3}$$

holds for all symmetric tensors e_{ij}. The problem $\mathcal{D}_1$ is solvable when the conditions

$$\int\limits_{\partial\Omega} P_i \,\mathrm{d}S = 0, \quad \int\limits_{\partial\Omega} (x \times P)_i \,\mathrm{d}S = 0 \tag{4}$$

are met. This problem is not uniquely solvable and it has infinite number of solutions. If $u_1(x)$ and $u_2(x)$ are two solutions then

$$u_2(x) - u_1(x) = Ax + b, \tag{5}$$

where A is an antisymmetric matrix 3×3 and b is a vector from R^3. This problem can be modified so that it will be uniquely solvable and this solution will be the minimum of the functional (1), i.e., the solution of the problem $\mathcal{D}_1$, provided the conditions (4) are met.

Let us define functionals on V

$$\begin{aligned} g_\alpha(u) &= \int\limits_\Gamma u_\alpha \,\mathrm{d}S, \quad \alpha = 1, 2, 3, \\ g_\alpha(u) &= \int\limits_\Gamma (x \times u)_{\alpha-3} \,\mathrm{d}S, \quad \alpha = 4, 5, 6. \end{aligned} \tag{6}$$

Then there is a constant $C > 0$ such that the following inequality

$$C \parallel u \parallel_V \leq \int\limits_{\Omega_1} c_{ijkl} e_{ij} e_{kl} \,\mathrm{d}x + g_\alpha(u) g_\alpha(u) \tag{7}$$

holds for all $u \in V$.

Let us formulate the second variational problem $\mathcal{D}_2$ whose solution is a minimum of the functional

$$\frac{1}{2} \int\limits_{\Omega_1} c_{ijkl} e_{ij}(u) e_{kl}(u) \,\mathrm{d}x + \frac{1}{2} g_\alpha(u) g_\alpha(u) - \int\limits_{\partial\Omega} P_i u_i \,\mathrm{d}S, \tag{8}$$

on V. The minimum of functional (8) is unique. Moreover the following inequality

$$\| u \|_V \leq C \| P \|_{[L^2(\partial\Omega)]^3} \tag{9}$$

holds, where C is a positive constant independent of u and P. The last inequality expresses the continuous dependence of the solution of the problem $\mathcal{D}_2$ on the force boundary conditions. Note that solving the problem $\mathcal{D}_2$ does not require the equilibrium conditions (4) to be met. But if these conditions are satisfied, the solution of $\mathcal{D}_2$ is a solution of $\mathcal{D}_1$. All these results can be found in the book [7].

Let τ_{ij} be a symmetric tensor. We say that the force boundary conditions P_i are generated by the tensor τ_{ij} when at every $x \in \partial\Omega$ the equation

$$P_i(x) = \tau_{ij} n_j(x) \tag{10}$$

holds, where $n_j(x)$ is a normal to the boundary $\partial\Omega$ at the point x.

Lemma 1. *Let τ_{ij} be a symmetric tensor and let P_i be defined by the formula (10) on the boundary $\partial\Omega$, then P_i satisfy the equilibrium conditions (4).*

Proof. If we use the Gaussian theorem on the surface integral, then

$$\int_{\partial\Omega} P_i(x)\,\mathrm{d}S = \int_{\partial\Omega} \tau_{ij} n_j(x)\,\mathrm{d}S = \int_{\Omega} \frac{\partial \tau_{ij}}{\partial x_j}\,\mathrm{d}x.$$

Since τ_{ij} is constant, then the last integral is zero. We express the formula $x \times P$ in the individual components, then

$$\begin{aligned}(x \times P)_1 &= x_2\tau_{3j}n_j - x_3\tau_{2j}n_j,\\ (x \times P)_2 &= x_3\tau_{1j}n_j - x_1\tau_{3j}n_j,\\ (x \times P)_3 &= x_1\tau_{2j}n_j - x_2\tau_{1j}n_j,\end{aligned}$$

where $n = (n_1, n_2, n_3)$ is the normal to the boundary $\partial\Omega$ at x. If we use the Gaussian theorem on the surface integral, then

$$\int_{\partial\Omega} (x \times P)_1\,\mathrm{d}S = \int_{\partial\Omega} x_2\tau_{3j}n_j - x_3\tau_{2j}n_j\,\mathrm{d}S = \int_{\Omega} \frac{\partial(x_2\tau_{3j} - x_3\tau_{2j})}{\partial x_j}\,\mathrm{d}x.$$

Since τ_{ij} is symmetric and constant, then the last integral is zero. The same equations can be proved for the components $(x \times P)_2$ and $(x \times P)_3$. □

The inequality (9) implies the existence of a continuous mapping

$$K\colon S^{\mathrm{sym}} \longrightarrow V, \tag{11}$$

where S^{sym} is the set of all second oder symmetric tensors. This mapping assigns a solution to the problem $\mathcal{D}_2$ to each second order symmetric tensor. Lemma 1 indicates that the value of this mapping is also a solution to the problem $\mathcal{D}_1$.

The following lemma will be useful in formulating the problem for determining the initial stress tensor.

Lemma 2. *Let* $u_1, u_2, x_1, x_2 \in R^3$ *and the value*

$$a = \frac{\|u_1 - u_2\|}{\|x_1 - x_2\|} < 1$$

be such small that a^2 *can be neglected, then the following equality*

$$\|u_1 + x_1 - u_2 - x_2\| - \|x_1 - x_2\| = \frac{\langle u_1 - u_2, x_1 - x_2\rangle}{\|x_1 - x_2\|}$$

holds approximately, where $\langle \cdot, \cdot \rangle$ *is the scalar product in* R^3*. Moreover, if*

$$v_1 = u_1 + Ax_1 + b, \qquad v_2 = u_2 + Ax_2 + b,$$

where A *is an antisymmetric matrix* 3×3 *and* b *is a vector from* R^3*, then*

$$\frac{\langle v_1 - v_2, x_1 - x_2\rangle}{\|x_1 - x_2\|} = \frac{\langle u_1 - u_2, x_1 - x_2\rangle}{\|x_1 - x_2\|}.$$

The proof of this lemma can be found in [8].

3. Description of the method

The method will be described on the geometry of two intersecting tunnels, which correspond to the real situation when the original stress tensor was determined. The situation is shown in Figures 2–4.

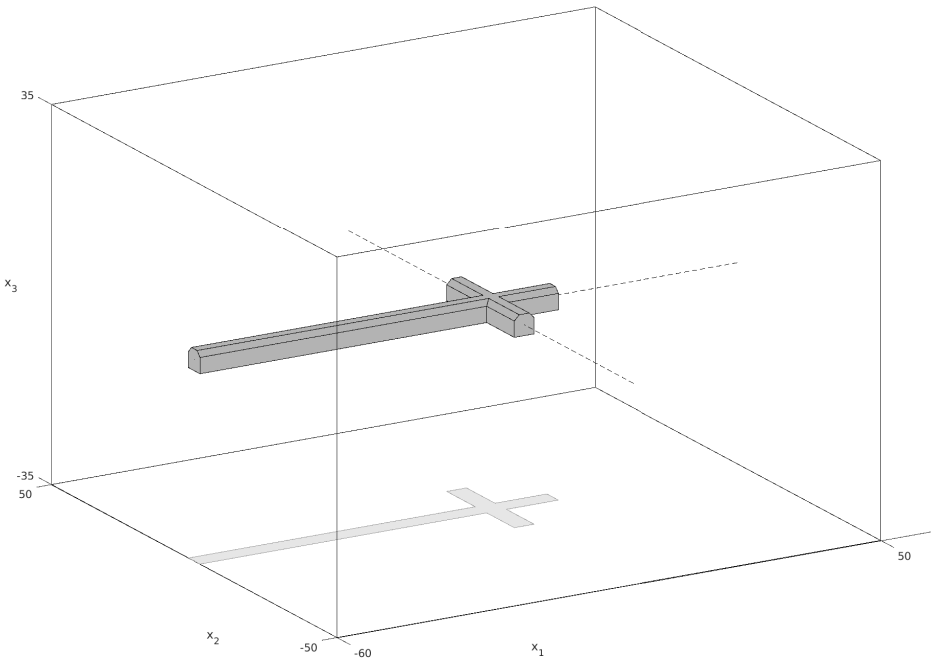

Figure 2: Underground opening in homogeneous domain Ω.

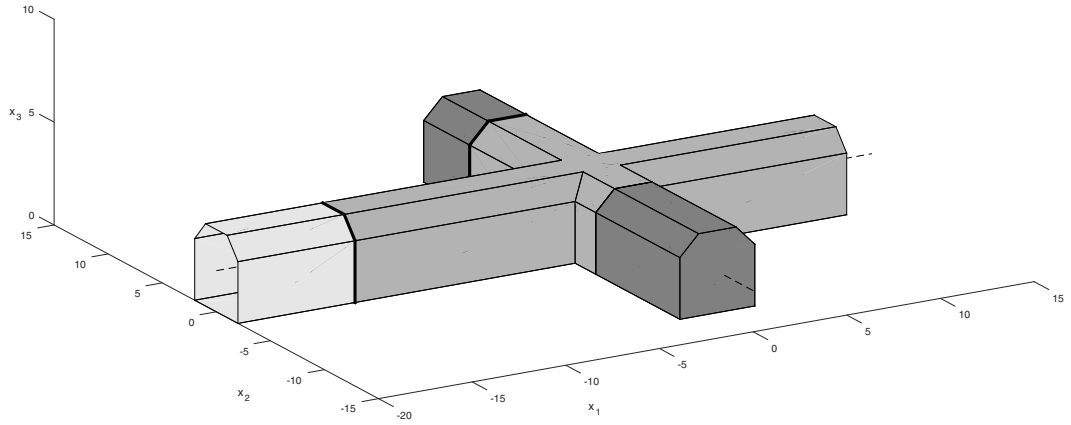

Figure 3: Detail of underground opening with highlighted three steps of the excavation process.

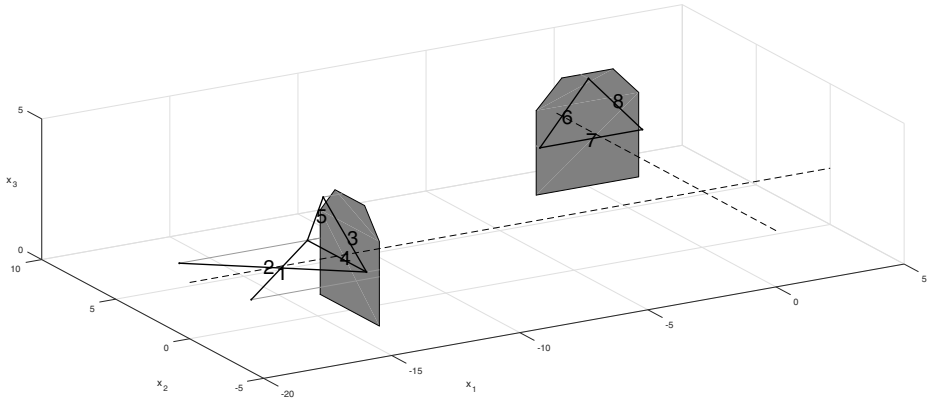

Figure 4: The pairs of measuring points corresponding to the highlighted faces of the tunnels from Figure 2.

Figure 2 shows the domain, where the underground opening is located, Figure 3 shows three steps of the excavation process. Highlighted faces of the tunnels indicate the location of the measuring points. Figure 4 shows the position of the pairs of measuring points to the highlighted faces from Figure 3. The set of the pairs of measuring points is divided into the two subsets $I_1 = \{1, 2, 3, 4, 5\}$ and $I_2 = \{6, 7, 8\}$.

Let Ω be the domain that corresponds to the prism shown in Figure 2. Let Ω_1, Ω_2, Ω_3 be the subdomains derived from the domain Ω by extraction of the parts corresponding to three steps of the excavation process shown in Figure 3.

In *Step* 1 (light gray color in Figure 3) the measuring points are installed on the walls of the tunnel and the distances between the selected pairs I_1 of measuring points are measured, see pairs $1, 2, 3, 4, 5$ in Figure 4. These measuring points are located at the ends of short steel bars, which are glued to the rock on the walls of the tunnel.

In *Step* 2 (medium gray color in Figure 3) another part of the main tunnel and a part of the tunnel oriented perpendicular to the main tunnel are excavated. The distances between the pairs I_1 are re-measured. The values obtained in *Step* 1 are subtracted from the values measured in *Step* 2 and the resulting values are marked d_i, $i \in I_1$. Moreover, another group of measuring points is installed on the walls of the tunnel perpendicular to the main tunnel – pairs 6, 7, 8 in Figure 4. The distances between the selected pairs I_2 of points are measured.

In *Step* 3 (dark gray color in Figure 3) remaining part of the perpendicular tunnel is extracted and then the distances in the second set I_2 of pairs of measuring points are re-measured. The values obtained in *Step* 2 are subtracted from the values measured in *Step* 3 and the resulting values are marked d_j, $j \in I_2$. The procedure for selecting the pairs of measuring points will be described below. We now explain how to obtain the initial stress tensor from these measurements.

Let's approach the formulation of our task. Let τ_{ij} be a symmetric second-order tensor that corresponds to the original stress tensor. We say that the force boundary conditions $\mathbf{P} = (P_1, P_2, P_3)$ are generated at the boundary of the domain by this tensor if

$$P_i(\mathbf{x}) = \tau_{ij} n_j(\mathbf{x}) \tag{12}$$

holds, where $\mathbf{n}(\mathbf{x})$ is the normal to the boundary of the domain at the point $\mathbf{x}$.

Assume that we know the solutions $\mathbf{u}_1(\mathbf{x}), \mathbf{u}_2(\mathbf{x}), \mathbf{u}_3(\mathbf{x})$ of the problem (1) on Ω_1, Ω_2, Ω_3 with the force boundary conditions given by the expression (12) on $\partial\Omega$ and be equal to zero of the remainders of the boundaries $\partial\Omega_1$, $\partial\Omega_2$, $\partial\Omega_3$. Due to Lemma 1 the solutions exist. Let the pairs of the points $\mathbf{x}_i, \mathbf{y}_i$, $i \in I_1$ in the first set and the pairs $\mathbf{x}_j, \mathbf{y}_j$, $j \in I_2$ in the second set be selected and the calculated differences in distances between these points are compared with numbers d_i, $i \in I_1$ and d_j, $j \in I_2$. These numbers represents the differences in the distances measured in the excavation process. The differences are equal to the following expressions

$$\begin{aligned} \|\mathbf{u}_2(\mathbf{x}_i) + \mathbf{x}_i - \mathbf{u}_2(\mathbf{y}_i) - \mathbf{y}_i\| - \|\mathbf{u}_1(\mathbf{x}_i) + \mathbf{x}_i - \mathbf{u}_1(\mathbf{y}_i) - \mathbf{y}_i\| = d_i, \quad i \in I_1, \\ \|\mathbf{u}_3(\mathbf{x}_j) + \mathbf{x}_j - \mathbf{u}_3(\mathbf{y}_j) - \mathbf{y}_j\| - \|\mathbf{u}_2(\mathbf{x}_j) + \mathbf{x}_j - \mathbf{u}_2(\mathbf{y}_j) - \mathbf{y}_j\| = d_j, \quad j \in I_2. \end{aligned} \tag{13}$$

In geo-mechanical practice, the displacements $\|\mathbf{u}(\mathbf{x}) - \mathbf{u}(\mathbf{y})\|$ is much smaller than $\|\mathbf{x} - \mathbf{y}\|$. Under these assumptions and Lemma 2, the relations (13) can be rewritten into the following form

$$\begin{aligned} \frac{\langle \mathbf{u}_2(\mathbf{x}_i) - \mathbf{u}_2(\mathbf{y}_i), \mathbf{x}_i - \mathbf{y}_i \rangle}{\|\mathbf{x}_i - \mathbf{y}_i\|} - \frac{\langle \mathbf{u}_1(\mathbf{x}_i) - \mathbf{u}_1(\mathbf{y}_i), \mathbf{x}_i - \mathbf{y}_i \rangle}{\|\mathbf{x}_i - \mathbf{y}_i\|} = d_i, \quad i \in I_1, \\ \frac{\langle \mathbf{u}_3(\mathbf{x}_j) - \mathbf{u}_3(\mathbf{y}_j), \mathbf{x}_j - \mathbf{y}_j \rangle}{\|\mathbf{x}_j - \mathbf{y}_j\|} - \frac{\langle \mathbf{u}_2(\mathbf{x}_j) - \mathbf{u}_2(\mathbf{y}_j), \mathbf{x}_j - \mathbf{y}_j \rangle}{\|\mathbf{x}_j - \mathbf{y}_j\|} = d_j, \quad j \in I_2, \end{aligned} \tag{14}$$

what is proved in [8]. Moreover the equations (14) are more suitable for further analysis and all mathematical aspects are also explained in [8]. The symbol $\langle \mathbf{x}, \mathbf{y} \rangle = x_i y_i$ in the expression (14) is the scalar product in R^3.

Now let's focus on finding the original stress tensor and consider the following six stress tensors.

$$\tau_{ij}^1 = \begin{pmatrix} 1 & 0 & 0 \\ 0 & 0 & 0 \\ 0 & 0 & 0 \end{pmatrix}, \quad \tau_{ij}^2 = \begin{pmatrix} 0 & 0 & 0 \\ 0 & 1 & 0 \\ 0 & 0 & 0 \end{pmatrix}, \quad \tau_{ij}^3 = \begin{pmatrix} 0 & 0 & 0 \\ 0 & 0 & 0 \\ 0 & 0 & 1 \end{pmatrix},$$

$$\tau_{ij}^4 = \begin{pmatrix} 0 & 1 & 0 \\ 1 & 0 & 0 \\ 0 & 0 & 0 \end{pmatrix}, \quad \tau_{ij}^5 = \begin{pmatrix} 0 & 0 & 1 \\ 0 & 0 & 0 \\ 1 & 0 & 0 \end{pmatrix}, \quad \tau_{ij}^6 = \begin{pmatrix} 0 & 0 & 0 \\ 0 & 0 & 1 \\ 0 & 1 & 0 \end{pmatrix}.$$

Next, let us denote $\mathbf{u}_1^k(\mathbf{x})$, $\mathbf{u}_2^k(\mathbf{x})$, $\mathbf{u}_3^k(\mathbf{x})$, $k = 1, \ldots, 6$ the solutions of the boundary value problems of the theory of elasticity on the domains Ω_1, Ω_2, Ω_3 with the force boundary conditions given by the tensors τ_{ij}^k using the relation (3) on $\partial\Omega$. The forces prescribed on $\partial\Omega_1 - \partial\Omega$, $\partial\Omega_2 - \partial\Omega$, $\partial\Omega_3 - \partial\Omega$, which corresponds to the walls of the gradually excavated tunnels, are zero.

As far as we use linear elastic model, we assume, that resulting displacements are linear combination of the displacements induced by auxiliary problems. So, the solution to our problem is the vector $\mathbf{z} = (z_1, z_2, z_3, z_4, z_5, z_6)$ such that the functions

$$\mathbf{u}_1(\mathbf{x}) = z_k \mathbf{u}_1^k(\mathbf{x}), \quad \mathbf{u}_2(\mathbf{x}) = z_k \mathbf{u}_2^k(\mathbf{x}), \quad \mathbf{u}_3(\mathbf{x}) = z_k \mathbf{u}_3^k(\mathbf{x})$$

satisfy the relations (5) and the tensor

$$\tau_{ij} = z_k \tau_{ij}^k \tag{15}$$

is the original stress tensor. To simplify further analysis, we will use the following designations

$$\begin{aligned} h_i^k &= \frac{\langle \mathbf{u}_2^k(\mathbf{x}_i) - \mathbf{u}_2^k(\mathbf{y}_i), \mathbf{x}_i - \mathbf{y}_i \rangle}{\|\mathbf{x}_i - \mathbf{y}_i\|} - \frac{\langle \mathbf{u}_1^k(\mathbf{x}_i) - \mathbf{u}_1^k(\mathbf{y}_i), \mathbf{x}_i - \mathbf{y}_i \rangle}{\|\mathbf{x}_i - \mathbf{y}_i\|}, \quad i \in I_1, \\ h_j^k &= \frac{\langle \mathbf{u}_3^k(\mathbf{x}_j) - \mathbf{u}_3^k(\mathbf{y}_j), \mathbf{x}_j - \mathbf{y}_j \rangle}{\|\mathbf{x}_j - \mathbf{y}_j\|} - \frac{\langle \mathbf{u}_2(\mathbf{x}_j) - \mathbf{u}_2(\mathbf{y}_j), \mathbf{x}_j - \mathbf{y}_j \rangle}{\|\mathbf{x}_j - \mathbf{y}_j\|}, \quad j \in I_2, \end{aligned} \tag{16}$$

which are connected with the relations (14). It is possible to use the least squares method that was proposed in [8], but now we will use a simpler method. Let us choose the set $J = J_1 \cup J_2$ such that $J_1 \subset I_1$, $J_2 \subset I_2$ and the number of elements of the set J is six. The vector $\mathbf{z}$ is a solution of the system of linear equations

$$\mathbf{H}\mathbf{z} = \mathbf{d}, \tag{17}$$

where the elements of 6×6 matrix $\mathbf{H} = (h_j^k)$, $1 \le k \le 6$, $j \in J$, we can find according to (16) and the components of the vector $\mathbf{d}$ are results of the measuring process described in *Step* 1–*Step* 3 for $j \in J$.

After solving the system (17), the initial stress tensor can be expressed in the form (15). It is very important to install pairs of measuring points so that the matrix $\mathbf{H}$ has favorable properties for solving the problem. Note that in the case of an insulated tunnel that does not intersect another tunnel, we could not find the location of the measuring points so that the matrix $\mathbf{H}$ has favorable properties. We will deal with this issue in the following section.

4. Optimal choice of measuring points

In this section, we will deal with the question of how to select pairs of points so that the system (17) has good properties from the point of view of the solvability of the problem. We select a pair of measuring points so that the matrix $\mathbf{H}$, which is constructed using formulas (16), has the property that a small change of the vector $\mathbf{d}$, the right side of the system (17), does not have much effect on the solution. This property is connected to the condition number $\kappa(\mathbf{H})$ of the matrix $\mathbf{H}$, which is expressed by the following formula

$$\kappa(\mathbf{H}) = \|\mathbf{H}\|\|\mathbf{H^{-1}}\|, \tag{18}$$

where $\|\mathbf{H}\|$ is the matrix norm of the matrix $\mathbf{H}$ and $\mathbf{H^{-1}}$ is the inverse matrix to $\mathbf{H}$. Then the relationship between the change of the solution $\delta\mathbf{z}$ of the system (16) and the change of the right side $\delta\mathbf{d}$ can be expressed by the following formula

$$\frac{\|\delta\mathbf{z}\|}{\|\mathbf{z}\|} \leq \kappa(\mathbf{H})\frac{\|\delta\mathbf{d}\|}{\|\mathbf{d}\|}.$$

The last inequality implies that for the reliability of the solution of the system (17) it is necessary that the condition number (18) is as small as possible. These results can be found in textbooks of linear algebra, for example in [9]. When we look at the way the matrices $\mathbf{H}$ are constructed using the expressions (16), we find that by a suitable choice of pairs of measuring points we are able to influence the condition number. The optimal distribution of measuring points is achieved by solving several auxiliary problems of the theory of elasticity and choosing a finite set of measuring points at the boundary of the underground opening. Then we select different sets of pairs of measuring points and check the value of the condition number of the matrix $\mathbf{H}$ composed of these pairs. As an optimal selection, we choose the set of pairs of measuring points for which the conditional number of the matrix $\mathbf{H}$ is the smallest. The selection of this set is based on mathematical modeling and specific cases will be analyzed in the next section. Note that if we can find the pairs of measuring points so that the conditional number of the corresponding matrix is less than 10 and we are able to guarantee a measurement accuracy of 1%, then the original stress tensor obtained by the methods described above will differ from the actual original stress tensor by 10 %.

We can say that the optimal selection of pairs of measuring points eliminates the effect of measurement errors. When applying the above method, we proceed as follows. We approximate the domains, shown in Figures 2–3 by finite element mesh and solve 18 auxiliary problems as described in Section 2. Then we select six pairs of points – nodes of the finite element mesh, compile the matrix and calculate the conditional number of this matrix. It is necessary to choose six pairs of points as far as the stress tensor has six independent components. We are looking for pairs of points on the walls of the underground opening so that it is possible to measure the distance between these points. We pass all suitable pairs of points and select the six pairs of points for which the conditional number of the matrix $\mathbf{H}$ is the smallest.

We will test this procedure on a pair of perpendicular vertical tunnels in the following section. We selected eight pairs of points as shown in Figure 4 and from this set we selected six pairs of points to show that the conditional number of the matrix depends on this selection. This procedure can be applied to various shapes of underground openings and mining operations. The shape of the underground opening and the excavation process were chosen in accordance with the research plan at the Bukov locality in the Czech Republic. This site serves as an underground laboratory and model repository for radioactive waste and is described in the report [11]. If we know the future shape of the underground opening and the progress of the mining work, we can use mathematical modeling, as described above, to select six pairs of measuring points in a suitable way and determine the tensor of the original stress.

We tried to apply this procedure to a direct tunnel and two steps of mining operations, but we were unable to find six pairs of measuring points so that the conditional number of the matrix $\mathbf{H}$ would be less than 60.

5. In situ experiment

The above-mentioned underground laboratory is located in a metamorphic rock, which is considered isotropic and homogeneous in the vicinity of the underground opening. The elastic properties of this rock are known from laboratory measurements, namely Yong's modulus $E = 60\,\mathrm{GPa}$ and Poisson's ratio $\mu = 0.25$. The expected shape of the underground opening and the progress of the mining works were known, which corresponds to Figure 2. Block Ω, into which two intersecting tunnels are nested, has dimensions $110\,\mathrm{m} \times 100\,\mathrm{m} \times 70\,\mathrm{m}$. The diameter of the tunnels is 4 m. The tunnel in the x_1 direction is long 70 m and the tunnel in the x_2 direction is long 30 m.

The GEM program, see [10], was used for analysis of the planned in situ experiment. The program has been developed at Institute of Geonics for solving geomechanical problems and allows solving elastic problems with force boundary conditions. The program has been used to solve 18 auxiliary problems as described in Section 3. However, it is possible to use any commercial program that allows you to solve such tasks.

A MATLAB program was written that tested all six possible pairs of points that were on the walls of the underground opening and the points were nodes of the finite element mesh used to solve the auxiliary problems. To demonstrate that the conditional number strongly depends on the selection of six pairs of measuring points, we selected six pairs of points from a set of eight elements, as shown in Figure 4. Six pairs from an eight-element set can be selected in twenty-eight ways. The results of this analysis are shown in Table 1. The selection is realized by two subsets $J_1 \subset I_1$ and $J_2 \subset I_2$, as described in Section 3. The configurations of the pairs of measuring points **c1** and **c2** correspond to the results with the two smallest conditional numbers of the matrix $\mathbf{H}$ and the configurations **c3** and **c4** correspond to the results with the two largest conditional numbers. The values of the conditional numbers are on the last line of Table 1.

c1		**c2**		**c3**		**c4**	
J_1	J_2	J_1	J_2	J_1	J_2	J_1	J_2
1,2,3	6,7,8	1,2,5	6,7,8	1,2,3,4	6,7	3,4,5	6,7,8
4.43		4.95		393.16		839.21	

Table 1: Selection of subsets J_1, J_2 and corresponding conditional numbers $\kappa(\mathbf{H})$.

d_1	d_2	d_3	d_4	d_5	d_6	d_7	d_8
-2.88	-0.60	-2.46	-5.32	-1.04	-1.75	-3.90	-2.79

Table 2: Measured differences in deformations in excavation process in [mm].

After this analysis, measurements were performed on selected pairs of measuring points in the corresponding steps of the mining process, as shown in Figures 2–3. The results of these measurements are shown in Table 2. The indexes at the numbers d_i correspond to the indexes of the pairs of measuring points as shown in Figure 4. The measuring points were placed at the ends of 60 cm long steel anchors, which were fixed in the rock with LOKSET ampules with polyester resin. The distances between the points were measured with a tape extensometer. This extensometer makes possible to measure distances between points with an accuracy of 0.01 mm. Considering the measured values in Table 2, the resolution of the extensometer guarantees a measurement accuracy of 1%.

The calculation was then performed, and the components of the original stress tensors τ_{ij} with the main stresses λ_i are shown in Table 3. The tensors thus obtained are shown in the principal stresses in Figure 5.

	τ_{11}	τ_{22}	τ_{33}	τ_{12}	τ_{23}	τ_{13}	λ_1	λ_2	λ_3
c1	-69.1	-95.6	-64.5	-70.0	10.7	13.3	-156.6	-61.7	-10.9
c2	-70.2	-94.8	-69.5	-63.1	-12.2	12.8	-146.8	-74.9	-12.8
c3	-12.5	-8.5	306.0	-47.7	-68.6	-100.8	-94.6	36.3	343.4
c4	-182.5	-12.6	143.0	-6362.7	588.6	656.9	-6576.3	258.3	6266.0

Table 3: Original stress tensor τ_{ij} and principal stresses λ_i in [MPa].

The directions of the principal stresses in the form of the unit eigenvectors $\mathbf{n}_1$, $\mathbf{n}_2$, $\mathbf{n}_3$ of the matrix $\mathbf{H}$ are shown in Table 4.

From Figure 5 and Tables 3–4, we can see that the tensors corresponding to the configurations **c1** and **c2** differ by about 10%, which is consistent with the hypothesis formulated in Section 4.

The configurations of pairs of measuring points **c3** and **c4** leads to very unlikely results, which corresponds very well to the fact that the conditional number of the matrix is large, as can be seen from Table 1.

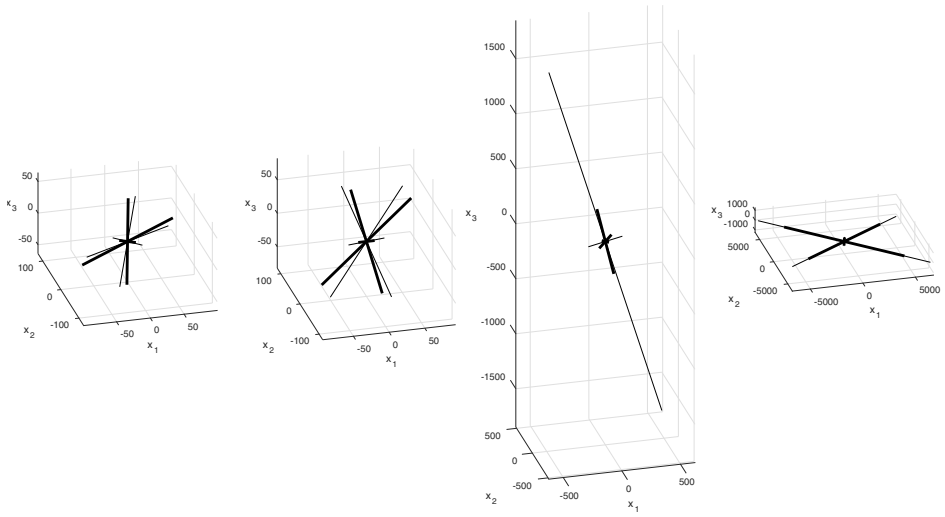

c1 **c2** **c3** **c4**

Figure 5: The original stress tensors in principal stresses and directions obtained by analysis of the configurations **c1**–**c4** of measurements. Bold lines – full precision of measured differences from Table 2 is used. Thin lines – measured values rounded to milimeters are used.

c1			**c2**		
$\mathbf{n}_1$	$\mathbf{n}_2$	$\mathbf{n}_3$	$\mathbf{n}_1$	$\mathbf{n}_2$	$\mathbf{n}_3$
-0.630	0.063	0.773	-0.630	-0.240	-0.730
-0.750	0.179	-0.630	-0.770	0.176	0.609
0.178	0.982	0.066	-0.010	0.955	-0.290
c3			**c4**		
$\mathbf{n}_1$	$\mathbf{n}_2$	$\mathbf{n}_3$	$\mathbf{n}_1$	$\mathbf{n}_2$	$\mathbf{n}_3$
0.721	0.646	-0.250	-0.706	0.088	-0.703
0.630	-0.760	-0.152	-0.696	0.096	0.712
0.289	0.048	0.956	0.130	0.992	-0.007

Table 4: Principal stress vectors.

The dependence of the stability of numerical solutin on the condition number we can see from the Figure 5 and from the Table 5. When we round the measured values in Table 2 to whole milimeters, tensors for configurations **c1** and **c2** changed slightly and tensors for configurations **c3** and **c4** changed significantly, which is also in line with the hypothesis formulated in Section 4.

Table 5 shows the differences

$$\Delta d = \frac{|d - \hat{d}|}{|d|}, \quad \Delta\tau = \frac{|\tau - \hat{\tau}|}{|\tau|},$$

	c1	**c2**	**c3**	**c4**
Δd	0.11	0.09	0.10	0.08
$\Delta\tau$	0.13	0.14	6.78	0.45

Table 5: Sensitivity of the value of resulting stress tensor to input data.

where $\hat{d}$ are the approximated values form Table 2 rounded to the milimeters and $\hat{\tau}$ is the stress tensor for these approximated values for the configurations **c1**–**c4**.

At the Bukov site, it was impossible to use the over-coring method or the cone probe method, which are described in [1], [6]. The rock in the Bukov locality is granular with a grain size of several millimeters, which is comparable to the size of the sensors on the probes in the above-mentioned. The individual measurements performed by these methods showed completely different results. The method proposed in this article shows stability of tensors for configurations **c1** and **c2**, while the resulting tensors for configurations **c3** and **c4** are not applicable. At the same time, the reasons for this behavior were explained.

In addition, the principal stress directions for tensors in configirations **c1** and **c2** coincide with the principal stress directions obtained by the hydraulic fracturing method, see [11]. The tunnel is located 550 m below the surface and at the specific rock mass 2700 $\mathrm{kg\,m^{-3}}$ so the component of the initial stress tensor τ_{33} should be equal to 14.8 MPa. The Young's modulus E must be changed so that the component τ_{33} of the original stress tensor is equal to this value. In Table 6, the original stress tensors for configurations **c1** and **c2** are recalculated, and the corresponding Young's modulus values are in the last column.

	τ_{11}	τ_{22}	τ_{33}	τ_{12}	τ_{23}	τ_{13}	λ_1	λ_2	λ_3	E
c1	-15.8	-22.0	-14.8	-16.1	2.5	3.1	-36.0	-14.2	-2.5	13.8
c2	-15.4	-20.9	-14.8	-13.9	-2.7	2.8	-32.3	-16.5	-2.8	12.8

Table 6: Modified original stress tensor and principal stresses in [MPa] and reduced Young's modulus E in [GPa].

The Young's modulus values were measured in the laboratory on a completely homogeneous sample, so such a reduction in value is acceptable. Note that in our case, the x_1 axis is oriented west-east and the original stress tensors are in natural coordinates and need not be transformed. Given the previous discussion, we can accept tensors for configurations **c1** and **c2** in Table 6 as the original stress tensor. These tensors differ by 10%.

6. Conclusion

In this paper, the authors presented a new method for determining the original stress tensor. This method is based on measuring the distance between pairs of selected points located on the walls of the underground work in the process of

the excavation. Part of the method is a procedure for selecting pairs of measuring points so that the estimate of the original stress tensor is reliable. This method is applicable to coarse-grained and anisotropic rocks, where other methods are not so successful. The measurements themselves are easy to carry out and the main work is connected with the selection of pairs of measuring points and the evaluation of measurements, which is based on mathematical modeling.

The authors believe that this method will find application in the construction of new underground openings.

Acknowledgment: This research has been supported by Czech Science Foundation (GAČR) through project No. 19-11441S, by European Union's Horizon 2020 research and innovation programme under grant agreement number 847593, and by The Czech Radioactive Waste Repository Authority (SÚRAO) under grant agreement number SO2020-017.

References

[1] Hudson, J. A., Cornet, F. H., Christiansson, R.: ISRM suggested methods for rock stress estimation - Part 1: strategy for rock stress estimation. International Journal of Rock Mechanics and Mining Sciences **40** (2003), 991–998.

[2] Sjőberg, J., Christiansen, R., Hudson, J. A.: ISRM suggested methods for rock stress estimation - Part 2: overcoring methods. International Journal of Rock Mechanics and Mining Sciences **40** (2003), 999–1010.

[3] Haimson, B. C., Cornet, F. H.: ISRM suggested methods for rock stress estimation - Part 3: hydraulic fracturing (HF) and/or hydraulic testing of pre-existing fractures (HTPF). International Journal of Rock Mechanics and Mining Sciences **40** (2003), 1011–1020.

[4] Wiles, T. D., Kaiser, P. K.: In situ stress determination using the under-excavation technique-I. Theory. International Journal of Rock Mechanics and Mining Sciences **31** (5) (1994), 439–446.

[5] Wiles, T. D., Kaiser, P. K.: In situ stress determination using the under-excavation technique-II. Applications. International Journal of Rock Mechanics and Mining Sciences **31** (5) (1994), 447–456.

[6] Sugawara, K., Obara, Y.: Draft ISRM suggested method for in situ stress measurement using the compact conical-ended borehole overcoring (CCBO)technique. International Journal of Rock Mechanics and Mining Sciences **36** (1999), 307–322.

[7] Nečas, J., Hlaváček, I.: *Mathematical Theory of Elastic and Elasto-plastic Bodies: An Introduction*. Elsevier, 1981.

[8] Malík, J., Kolcun, A.: Determination of initial stress tensor from deformation of underground opening in excavation process. Appl. Math., accepted, available on line.

[9] Lax, P. D.: *Linear Algebra and Its Applications*. Wiley, 2007.

[10] Blaheta, R., Jakl, O., Kohut, R., Starý, J.: GEM – a platform for advanced mathematical geosimulations. In: R. Wyrzykowski (Ed.), *Proceedings of Parallel Processing and Applied Mathematics, Lecture Notes in Computer Science*, pp. 66–275. Springer-Verlag, 2010.

[11] Souček, K. et al.: *Comprehensive geological characterization of URF Bukov-part II Geotechnical characterization*. Final report 221/2018. SÚRAO, IG CAS, 2017, 109–121.